A Study of Composite Resonance in AC/DC Converters

S. R. Naidu, *Member, IEEE,* and Robert H. Lasseter, *Fellow, IEEE*

***Abstract*—Control-system errors and imbalances in the ac system may generate and magnify abnormal harmonics in the ac-bus voltages and the dc current. In this paper, a technique based on harmonic impedance matrices has been used to simulate the steady-state response of ac/dc converters. The technique allows the computation of converter impedances or admittances viewed from the dc or ac bus. At any operating point, a linear circuit may represent the converter and harmonic magnification factors are calculated. High harmonic magnification indicates the possibility of composite resonance. The impact of a small negative-sequence imbalance in the ac system voltages is shown for a six-pulse current-controlled converter.**

***Index Terms*—AC/DC converters, harmonic interaction, resonance.**

I. Introduction

WAVEFORM distortion in ac/dc converters has been very difficult to quantify and consequently, has not been well understood. It has been observed that converters with low short-circuit ratio experience high levels of waveform distortion. This has been attributed to the high ac system impedance, whose inductance may resonate with the capacitors and filters installed at the converter's ac terminals. Resonance of this nature may lead to harmonic instability.

The ac/dc converter is the interconnection of the ac and dc systems via the static converter. The ac system impedance interacts through the converter characteristics to present entirely different impedance to the dc side. This gives rise to resonance frequencies, which depend on the ac system impedance, the dc system impedance and the switching of the converter. The resonance is "composite," implying its dependence on all elements of the ac/dc converter.

Several contributions have appeared in the literature on harmonic instability but few have directly addressed the phenomenon of composite resonance. One of the earliest analyses of harmonic instability is reported in [1]. Harmonic instability related to firing-angle imbalance has been identified in this contribution and the concept of harmonic magnification is defined. In another study [2], the linear relationships between integer harmonics on both sides of the converter have been obtained numerically from the converter simulation. The converter control system has been included in the simulation and the overall harmonic impedances at both the ac and dc terminals are derived. The harmonic impedance has been used to predict lightly or negatively damped integer harmonics.

A technique based on the eigenvalue and frequency-domain approach has been used in [3] to analyze the low order harmonic instability. Approximate switching functions have been used in [4] to derive the small-signal model and to study harmonic interaction in a converter supplying an arc furnace. Transfer functions for the current-control loop of a HVDC link have been calculated in [5] and the stability of the system has been analyzed. Based on a simplified model of the commutation process, transfer functions that convert ac voltage to dc voltage and dc current to ac current have been derived in [6].

A frequency domain analysis has been used in [7] to obtain a set of simultaneous equations, which, after considerable manipulation, reduce to a matrix equation relating the ac and dc harmonics. The converter impedance seen by the dc system is derived from this equation. At this stage, the expression for the composite impedance becomes complicated. An equivalent RLC network is derived which matches the composite impedance at its resonant frequency. Composite resonance damping is taken to be identical to the damping factor of the equivalent RLC circuit.

It becomes clear that the composite impedance is essentially a matrix quantity. This is true for the composite impedances seen on the ac and dc sides of the converter. Any single harmonic component of current flowing into composite impedance produces a multitude of voltage harmonics. Some means for identifying the resonance frequencies becomes necessary. Amplification factors have been used [8] to isolate the resonant frequencies and these factors are defined as the transfer functions from a fictitious voltage source placed in series with the converter to the voltage across the dc filter.

In this paper, a technique based on the harmonic impedance matrix is used to determine the steady-state responses of a current-controlled six-pulse ac/dc converter. The simulation procedure is general and can include the frequency-dependence of parameters. The linear equivalent circuit of the converter is derived for each operating point and it has been used to compute the impedance (admittance) presented by the converter at its dc (ac) terminals. The impact of negative-sequence imbalance in the ac system voltages on the ac-bus voltage harmonics and dc current harmonics has been determined. All interactions have been computed using full matrices. Therefore, cross-frequency effects have been included.

Manuscript received August 12, 2002.

S. R. Naidu is with the Department of Electrical Engineering, Universidade Federal da Paraiba, Campina GrandePB 58109-970, Brazil (e-mail: naidu@dee.ufpb.br).

R. H. Lasseter is with the Department of Electrical and Computer Engineering, University of Wisconsin-Madison, Madison, WI 53706-1691 USA (e-mail: lasseter@engr.wisc.edu).

Digital Object Identifier 10.1109/TPWRD.2003.813612

II. Time-Domain Representation of Impedances

Consider a periodic waveform $x(t)$ of limited bandwidth. The time-domain representation of this waveform is $\boldsymbol{x}$, the n-vector of equidistant samples over one period at the fundamental frequency. The phasor-domain representation of the waveform is

$$\boldsymbol{X} = \boldsymbol{F} \cdot \boldsymbol{x} \tag{1}$$

where $\boldsymbol{F}$ is the $n \times n$, symmetric, complex matrix associated with the discrete Fourier transform [9].

The first element of $\boldsymbol{X}$ is the dc component of $x(t)$. The next m elements are the phasors representing the "m" harmonic components of $x(t)$, where $m = n/2 - 1$. The phasor component at the highest frequency is $X(m+2)$, which is real if $\boldsymbol{x}$ is a vector of real-valued samples. The subsequent m elements from $X(m+3)$ to $X(n)$ are the conjugates of $X(2)$ to $X(m+1)$ in reverse order [9]. The structure of $\boldsymbol{X}$ is therefore

$$\boldsymbol{X} = [\boldsymbol{X_{DC}}\ \boldsymbol{X}_1\ \boldsymbol{X}_2 \cdots \boldsymbol{X_{m+1}}\ \boldsymbol{X_{m+2}}\ \boldsymbol{X^*_{m+1}} \cdots \boldsymbol{X}^*_2\ \boldsymbol{X}^*_1]^{\boldsymbol{t}}. \tag{2}$$

Impedances of linear network branches are represented in the phasor-domain by $n \times n$-dimensional, complex, diagonal matrices and the diagonal of complex harmonic impedances has the same form as (2). Let $\boldsymbol{Z}$ be the complex impedance matrix of a linear network branch. Let $\boldsymbol{E}$, $\boldsymbol{I}(\boldsymbol{e}, \boldsymbol{i})$ be the phasor-domain (time-domain) representation of the periodic voltage and current waveforms associated with the impedance. Then

$$\boldsymbol{E} = \boldsymbol{Z} \cdot \boldsymbol{I}. \tag{3}$$

From (3), we obtain

$$\boldsymbol{e} = \boldsymbol{F}^{-1} \cdot \boldsymbol{Z} \cdot \boldsymbol{F} \cdot \boldsymbol{i} = \boldsymbol{z} \cdot \boldsymbol{i} \tag{4}$$

where $\boldsymbol{z}$ is the impedance matrix in the time domain. It is a real, full matrix having a circulant structure. The first column of $\boldsymbol{z}$ is the inverse discrete Fourier transform of the diagonal of $\boldsymbol{Z}$.

In contrast to the impedance matrix of a linear circuit, the time-domain conductance matrix of a thyristor switch is diagonal and the elements on the diagonal are the equidistant samples of the thyristor's conductance over a fundamental period. Let $\boldsymbol{g}$ be the diagonal conductance matrix of a thyristor switch and let $\boldsymbol{e}$ be the periodic voltage waveform across its terminals. Then the thyristor current waveform is

$$\boldsymbol{i} = \boldsymbol{g} \cdot \boldsymbol{e}. \tag{5}$$

From (5)

$$\boldsymbol{I} = \boldsymbol{F} \cdot \boldsymbol{g} \cdot \boldsymbol{F}^{-1} \cdot \boldsymbol{E} = \boldsymbol{G} \cdot \boldsymbol{E}. \tag{6}$$

$\boldsymbol{G}$ is the thyristor conductance matrix transformed to the phasor-domain. It is a full matrix, with the off-diagonal elements representing the cross-frequency coupling admittances. The elements on the diagonal are the harmonic self-admittances.

It should be noted that time-domain and phasor-domain convolutions are implicit in the construction of the matrices $\boldsymbol{z}$ and $\boldsymbol{G}$ [9].

III. Composite Resonance

The ac terminal of the converter is considered to be on the source side of the transformer's leakage reactance. The converter presents a set of admittances at its ac terminal, which depend on the dc system admittance, the transformer leakage inductance, and the conduction periods of the individual thyristors. These admittances are full complex matrices in the phasor-domain. On the other hand, the ac system admittances are complex diagonal matrices. The composite admittance at the ac terminal is the sum of the ac system admittance and the converter's ac-side admittance. The diagonal elements of the composite admittance matrix are the total harmonic self-admittances. AC-side composite resonance occurs when the imaginary part of a harmonic self-admittance vanishes.

The impedance presented by the converter at its dc terminal depends on the ac system impedance including the transformer leakage inductance, and the conduction periods of the thyristors. The dc-side converter impedance is a full, complex matrix. The dc system impedance is, however, a complex diagonal matrix. The composite impedance at the dc terminal is the sum of the dc system impedance and the converter's impedance. The diagonal elements of the composite impedance are the total harmonic self-impedances. DC-side composite resonance occurs when the imaginary part of a harmonic self-impedance is zero.

IV. Six-Pulse AC/DC Converter Analysis

Fig. 1(a) shows a three-phase, six-pulse ac/dc converter. The ac system consists of a source, its internal impedance, a shunt capacitor connected to the ac-bus and the leakage inductance of the transformer between the ac-bus and the input terminals of the thyristor bridge. The current controller shown in Fig. 1(b) has two parallel functions [10], a simple gain, and another response function to provide a gain related to the rate of change of current. The sum of the two functions is input to an integrator with gain, which computes the firing angle.

Two-state resistors model the thyristors. When conducting, a thyristor is assumed to have a resistance of 1 mΩ and this value jumps to 50 MΩ in the nonconducting state.

There are four unknown voltage waveforms to be determined. These are $\boldsymbol{e_{AB}}$, $\boldsymbol{e_{BC}}$, $\boldsymbol{e_{LD}}$ at the input and output terminals of the thyristor bridge and the voltage $\boldsymbol{v_N}$ of one of the thyristors. The equations for the unknown variables are obtained by applying Kirchhoff's current law at the nodes A, C and D. The fourth equation is obtained by equating the sum of the currents in the upper row of thyristors to the sum of the currents in the lower row of thyristors. These equations are nonlinear, since the thyristor conductance matrices depend on the unknown voltages and the switching instants. They are solved iteratively using the Newton–Raphson procedure. The computations involved are listed below.

Compute the admittance matrices $\boldsymbol{y_{AC}}$, $\boldsymbol{y_{DC}}$ of the ac and dc systems respectively and the short-circuit currents at the input terminals of the thyristor bridge. The short-circuit currents are $\boldsymbol{c_{AB}}$, $\boldsymbol{c_{BC}}$, $\boldsymbol{c_{CA}}$ for the phases AB, BC and CA. The matrix $\boldsymbol{y_{AC}}$ includes the leakage inductance of the transformer.

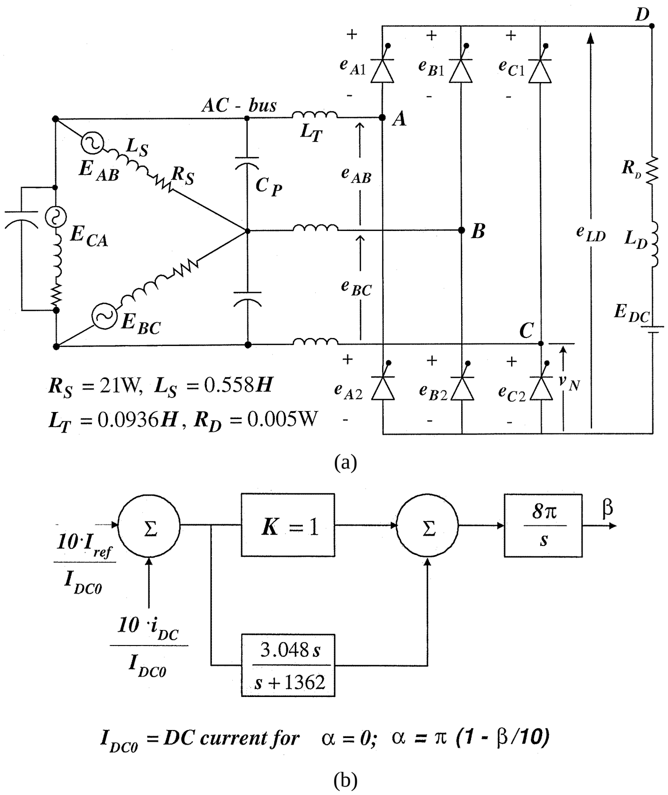

Fig. 1. (a) Three-phase ac/dc converter. (b) Current controller.

1. Assume the waveforms e_{AB}, e_{BC}, e_{LD} and v_N. Then, the thyristor voltages are

$$e_{A2} = e_{AB} + e_{BC} + v_N; \quad e_{B2} = e_{BC} + v_N; \quad e_{C2} = v_N;$$
$$e_{A1} = e_{LD} - e_{A2}; \quad e_{B1} = e_{LD} - e_{B2}; \quad e_{C1} = e_{LD} - e_{C2}.$$

2. Calculate the dc current waveform

$$j_{LD} = y_{DC} \cdot (e_{LD} - E_{DC}).$$

3. Using the waveform obtained in step 2 as input to the current controller, the firing instants for the thyristors are determined as described in [10].

4. The thyristor voltages obtained in step 1 and the switching instants calculated in step 3 permit the computation of the conduction periods and the diagonal conductance matrices of the thyristors. These are g_{A1}, g_{A2}, g_{B1}, g_{B2}, g_{C1}, g_{C2}.

5. Apply Kirchhoff's current law as described previously. Since the waveforms in step 1 are solution estimates, KCL will not be satisfied but will give the residual currents

$$(c_{AB} - c_{CA}) - y_{AC} \cdot e_{AB} - y_{AC} \cdot (e_{AB} + e_{BC}) - g_{A2} \cdot e_{A2} + g_{A1} \cdot e_{A1} = \delta j_{AB} \tag{7}$$

$$(c_{BC} - c_{CA}) - y_{AC} \cdot e_{BC} - y_{AC} \cdot (e_{AB} + e_{BC}) + g_{C2} \cdot e_{C2} - g_{C1} \cdot e_{C1} = \delta j_{BC} - \delta j_N \tag{8}$$

$$g_{A1} \cdot e_{A1} + g_{B1} \cdot e_{B1} + g_{C1} \cdot e_{C1} + y_{DC} \cdot (e_{LD} - E_{DC}) = -\delta j_{LD} \tag{9}$$

$$g_{A1} \cdot e_{A1} + g_{B1} \cdot e_{B1} + g_{C1} \cdot e_{C1} - g_{A2} \cdot e_{A2} - g_{B2} \cdot e_{B2} - g_{C2} \cdot e_{C2} = \delta j_N. \tag{10}$$

Note that (7)–(10) are matrix equations. These equations are written in the form

$$\begin{bmatrix} c_{AB} - c_{CA} \\ c_{BC} - c_{CA} \\ y_{DC} \cdot E_{DC} \\ 0 \end{bmatrix} - J \cdot \begin{bmatrix} e_{AB} \\ e_{BC} \\ e_{LD} \\ v_N \end{bmatrix} = \begin{bmatrix} \delta j_{AB} \\ \delta j_{BC} \\ \delta j_{LD} \\ \delta j_N \end{bmatrix}. \tag{11}$$

Putting

$$g_A = g_{A1} + g_{A2}, \quad g_B = g_{B1} + g_{B2}, \quad g_C = g_{C1} + g_{C2},$$
$$g_{AB} = g_{A1} + g_{B1}, \quad g_1 = g_{A1} + g_{B1} + g_{C1},$$
$$g_2 = g_{A2} + g_{B2} + g_{C2}, \quad g_3 = g_A + g_B$$

the Jacobian matrix J is given by

$$J = \begin{bmatrix} 2y_{AC} + g_A & y_{AC} + g_A & -g_{A1} & g_A \\ y_{AC} + g_A & 2y_{AC} + g_3 & -g_{AB} & g_3 \\ -g_{A1} & -g_{AB} & y_{DC} + g_1 & -g_1 \\ g_A & g_3 & -g_1 & g_1 + g_2 \end{bmatrix}. \tag{12}$$

6. The corrections δe_{AB}, δe_{BC}, δe_{LD}, δv_N that should be added to the assumed waveforms to minimize the residual currents are

$$\begin{bmatrix} \delta e_{AB} \\ \delta e_{BC} \\ \delta e_{LD} \\ \delta v_N \end{bmatrix} = J^{-1} \cdot \begin{bmatrix} \delta j_{AB} \\ \delta j_{BC} \\ \delta j_{LD} \\ \delta j_N \end{bmatrix}. \tag{13}$$

7. Return to step 1 if the maximum norm of the residuals is above a specified tolerance.

A. DC-Side Converter Impedance

Removing the ac and dc system excitations and substituting the thyristors by their respective conductance matrices gives the linear circuit representing the ac/dc converter at a given operating point. Let j_Z be a current injected into the dc terminals of the converter after disconnecting the dc system. The voltage e_Z developed at these terminals is obtained from

$$J_1 \cdot \begin{bmatrix} e_{AB} \\ e_{BC} \\ e_Z \\ v_N \end{bmatrix} = \begin{bmatrix} 0 \\ 0 \\ j_Z \\ 0 \end{bmatrix}. \tag{14}$$

The matrix J_1 is obtained from J by putting $y_{DC} = 0$ in its elements. By elimination, (14) may be reduced to

$$e_Z = z_C \cdot j_Z \tag{15}$$

where z_C is the time-domain impedance matrix for the converter at its DC terminals. Cross-frequency couplings are taken into account in this matrix. The corresponding harmonic domain matrix is given by

$$Z_C = F \cdot z_C \cdot F^{-1}. \tag{16}$$

The elements of Z_C are complex impedances.

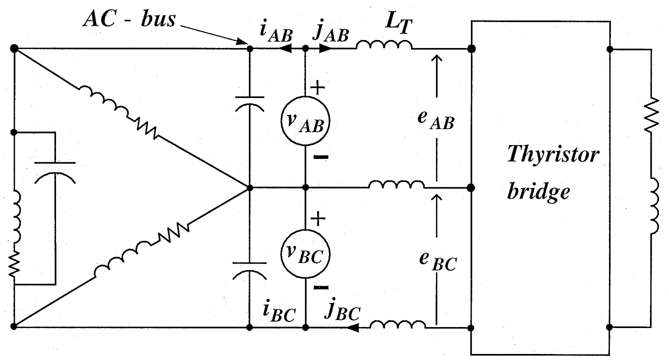

Fig. 2. AC-side representation of the converter.

B. DC-Side Harmonic Magnification Factors

Consider the converter at an operating point. The impact of a small negative-sequence imbalance may be calculated by using the linear converter circuit. It is assumed that the imbalance in the ac system excitation will not affect the switching of the thyristors.

Let $\boldsymbol{j}_0$ be the short-circuit current at the dc terminals of the linear circuit with the negative-sequence voltage as the ac-system excitation. Let $\boldsymbol{j_C}$ be the dc current when the dc system is connected to the converter. The magnification factor at the kth harmonic is defined as the ratio of the amplitudes of the kth harmonic of $\boldsymbol{j_C}$ to the corresponding amplitude of $\boldsymbol{j}_0$. The magnification factor depends on the relative phase of the negative-sequence voltage, which is random. Only the maximum magnification factor as the phase varies, is considered. A high magnification factor implies the possibility of composite resonance on the dc-side.

C. AC-Side Admittances

The transformer leakage inductances are usually included in the converter admittances viewed from the ac-bus. Let voltages $\boldsymbol{v_{AB}}, \boldsymbol{v_{BC}}$ be applied to the ac terminals of the converter, as shown in Fig. 2. Using the linear circuit of the converter at the operating point, the equations relating the converter currents and voltages are

$$\boldsymbol{J}_2 \cdot \begin{bmatrix} \boldsymbol{e_{AB}} \\ \boldsymbol{e_{BC}} \\ \boldsymbol{e_{LD}} \\ \boldsymbol{v_N} \end{bmatrix} = \begin{bmatrix} \boldsymbol{j_{AB}} \\ \boldsymbol{j_{BC}} \\ 0 \\ 0 \end{bmatrix} \tag{17}$$

where $\boldsymbol{J}_2$ is obtained from $\boldsymbol{J}$ by putting $\boldsymbol{y_{AC}} = 0$ in its elements. Eliminating $\boldsymbol{e_{LD}}, \boldsymbol{v_N}$ from (17)

$$\begin{bmatrix} \boldsymbol{j_{AB}} \\ \boldsymbol{j_{BC}} \end{bmatrix} = \begin{bmatrix} \boldsymbol{g}_{11} & \boldsymbol{g}_{12} \\ \boldsymbol{g}_{21} & \boldsymbol{g}_{22} \end{bmatrix} \cdot \begin{bmatrix} \boldsymbol{e_{AB}} \\ \boldsymbol{e_{BC}} \end{bmatrix}. \tag{18}$$

Let $\boldsymbol{z_T}$ be the impedance matrix for the transformer's leakage inductance. Then, from Fig. 2

$$\begin{bmatrix} \boldsymbol{v_{AB}} \\ \boldsymbol{v_{BC}} \end{bmatrix} = \begin{bmatrix} \boldsymbol{e_{AB}} \\ \boldsymbol{e_{BC}} \end{bmatrix} + \begin{bmatrix} 2 \cdot \boldsymbol{z_T} & \boldsymbol{z_T} \\ \boldsymbol{z_T} & 2 \cdot \boldsymbol{z_T} \end{bmatrix} \cdot \begin{bmatrix} \boldsymbol{j_{AB}} \\ \boldsymbol{j_{BC}} \end{bmatrix}. \tag{19}$$

From (18) and (19)

$$\begin{bmatrix} \boldsymbol{j_{AB}} \\ \boldsymbol{j_{BC}} \end{bmatrix} = \begin{bmatrix} \boldsymbol{y}_{11} & \boldsymbol{y}_{12} \\ \boldsymbol{y}_{21} & \boldsymbol{y}_{22} \end{bmatrix} \cdot \begin{bmatrix} \boldsymbol{v_{AB}} \\ \boldsymbol{v_{BC}} \end{bmatrix}. \tag{20}$$

The matrices $\boldsymbol{y}_{11}, \boldsymbol{y}_{12}, \boldsymbol{y}_{21}, \boldsymbol{y}_{22}$ give the converter admittances seen from the ac-bus.

The ac system is governed by

$$\begin{bmatrix} \boldsymbol{i_{AB}} \\ \boldsymbol{i_{BC}} \end{bmatrix} = \begin{bmatrix} 2 \cdot \boldsymbol{y'_{AC}} & \boldsymbol{y'_{AC}} \\ \boldsymbol{y'_{AC}} & 2 \cdot \boldsymbol{y'_{AC}} \end{bmatrix} \cdot \begin{bmatrix} \boldsymbol{v_{AB}} \\ \boldsymbol{v_{BC}} \end{bmatrix} \tag{21}$$

where $\boldsymbol{y'_{AC}}$ is the admittance matrix per phase of the ac system without the transformer's leakage inductance. The total admittance at the ac-bus is given by

$$\boldsymbol{y_{TOT}} = \begin{bmatrix} 2 \cdot \boldsymbol{y'_{AC}} & \boldsymbol{y'_{AC}} \\ \boldsymbol{y'_{AC}} & 2 \cdot \boldsymbol{y'_{AC}} \end{bmatrix} + \begin{bmatrix} \boldsymbol{y}_{11} & \boldsymbol{y}_{12} \\ \boldsymbol{y}_{21} & \boldsymbol{y}_{22} \end{bmatrix}. \tag{22}$$

D. AC-Side Harmonic Magnification Factors

Consider the linear circuit of the converter at an operating point and let the excitation be the negative-sequence voltages of amplitude δv_{NS}. Let $\delta \boldsymbol{V_{AB}}$ be the phasor representation of the ac-bus voltage waveform of phase AB. The ac-side harmonic magnification factors are defined as

$$\boldsymbol{m_{ac}} = (1/\delta \boldsymbol{v_{NS}}) \cdot \boldsymbol{abs}(\delta \boldsymbol{V_{AB}}). \tag{23}$$

Of particular interest is the fourth element of $\boldsymbol{m_{ac}}$ which is the magnification factor for the third harmonic. High values of this element indicate ac-side composite resonance at the third harmonic.

V. Results and Discussion

The six-pulse converter shown in Fig. 1(a) is used as the example for investigation. In all cases, the requested dc current for the controller is set at 60% of the current corresponding to $\alpha = 0$. The impact of 2% negative-sequence imbalance in the ac system voltages on the dc current and ac-bus voltage harmonics is the primary concern of this study.

The simulations used $n = 256$, which is convenient to use with the fast Fourier transform (FFT). A larger sampling frequency increases the solution time considerably. The simulations presented in this study are limited by this sampling frequency.

A. DC-Side Composite Resonance

Fig. 3 shows the 2nd harmonic magnification as a function of the shunt capacitance and it indicates a high gain when the capacitance is 1.89 μF. The smoothing inductance has been fixed at 0.6243 H. Fig. 4 confirms that the largest increase in the 2nd harmonic content of the dc current occurs when the shunt capacitance is 1.89 μF. Fig. 5 compares the dc current waveforms with and without the 2% negative-sequence imbalance.

As discussed in Section IV-A, the harmonic domain converter impedance matrix $\boldsymbol{Z_C}$ seen at the dc-bus is a full matrix whereas the dc system impedance matrix is a diagonal matrix. When the two matrices are added together, there could be a significant cancellation of the imaginary parts of the elements on the diagonal. Fig. 6 shows the real and imaginary parts of the converter's 2nd

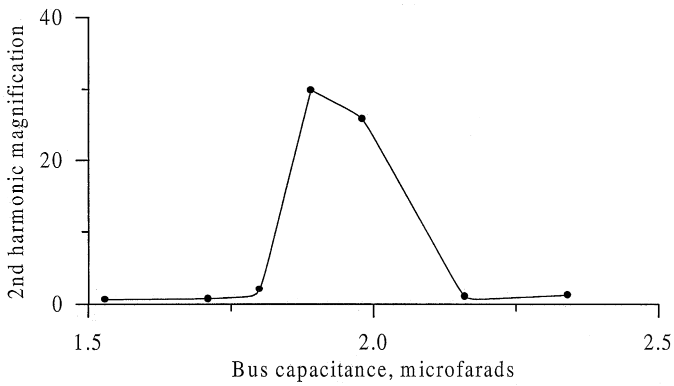

Fig. 3. DC-side 2nd harmonic magnification factors.

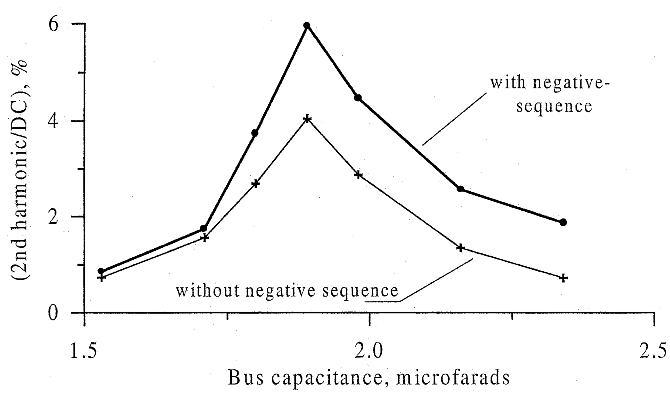

Fig. 4. (Second harmonic/dc) ratio of the dc current.

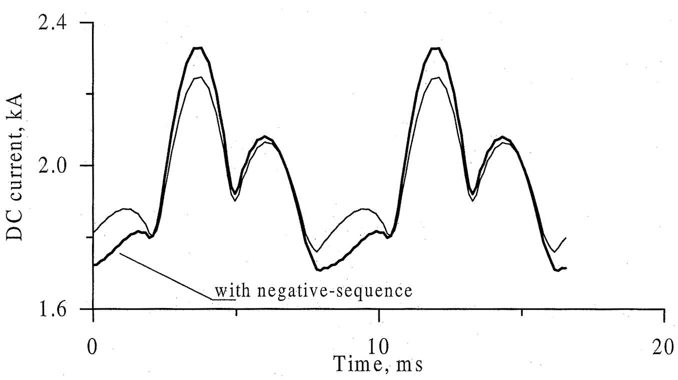

Fig. 5. Impact of 2% negative-sequence imbalance on dc current waveform.

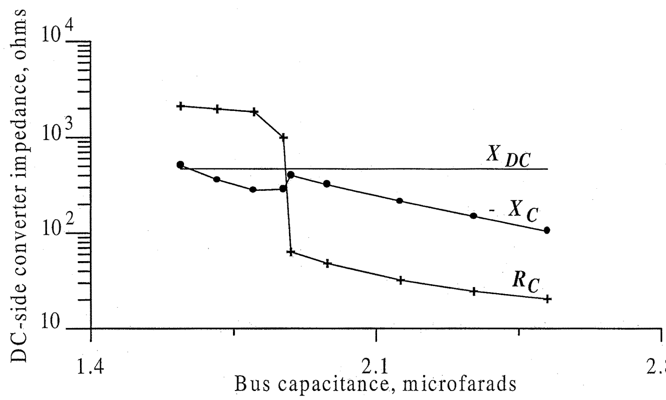

Fig. 6. DC-side converter impedance.

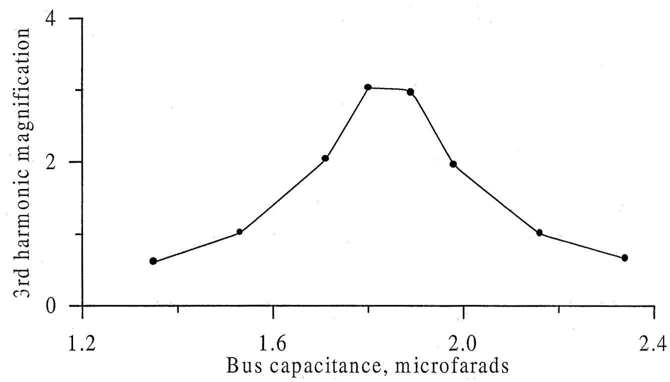

Fig. 7. AC-side 3rd harmonic magnification factors.

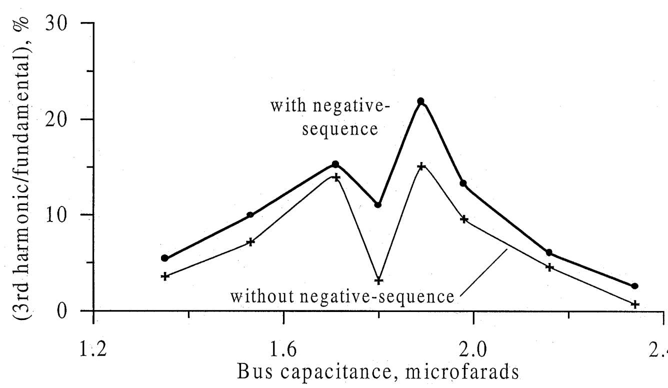

Fig. 8. (3rd harmonic/fundamental) ratio for ac-bus voltages. ($L_D = 0.6243$ H).

harmonic self-impedance $\boldsymbol{R_C} + \boldsymbol{jX_C}$ as a function of the shunt capacitance. This is the 3rd element on the diagonal of $\boldsymbol{Z_C}$. The same figure shows the constant reactance X_{DC} of the dc system. Though a total cancellation of the reactive parts is not observed, the total impedance at the 2nd harmonic is indeed a minimum at 1.89 μF.

The total impact of the negative-sequence imbalance is due to the transfer of the negative-sequence voltage to the dc-side as a 2nd harmonic voltage, as well as the cancellation of the reactive part of the total 2nd harmonic impedance. The harmonic magnification factor takes both effects into account.

B. AC-Side Composite Resonance

Fig. 7 shows the ac-side magnification factor at the 3rd harmonic when the shunt capacitance is varied. Maximum magnification is observed when the capacitance is 1.8 μF. Figs. 8 and 9 show the increase in the 3rd harmonic content of the ac-bus voltages when either the shunt capacitance or the smoothing inductance is varied. The impact of the 2% negative-sequence imbalance is a maximum when the capacitance is 1.8 μF and the inductance is 0.6243 H. Fig. 10 shows one of the ac-bus voltage waveforms for these parameter values.

The total admittance of the converter at the ac-bus (22) is the addition of four diagonal matrices representing the ac system to four full matrices representing the converter admittances seen

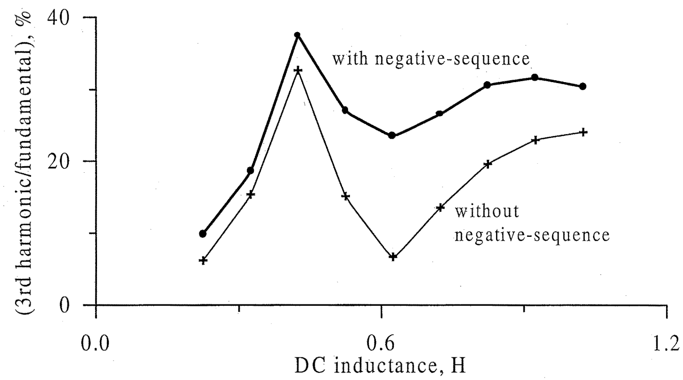

Fig. 9. (3rd harmonic/fundamental) ratio for ac-bus voltages. ($C_P = 1.8\ \mu$F).

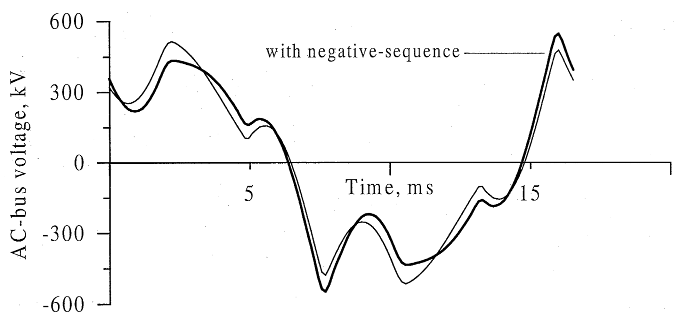

Fig. 10. Impact of 2% negative-sequence imbalance on ac-bus voltage waveform.

at the ac-bus. When the shunt capacitance is 1.8 μF and the smoothing inductance is 0.6243 H, the 3rd harmonic admittance of the ac system in (22) is $y'_{AC}(4, 4) = 0.000\,052\,7 + j0.000\,453$. The corresponding 3rd harmonic self-admittances for the converter are

$$y_{11} = 0.000\,03 - j0.000\,849, \quad y_{12} = 0.000\,194 - j0.000\,41$$
$$y_{21} = -0.000\,188 - j0.000\,409, \quad y_{22} = 0.000\,003 - j0.000\,85.$$

When added together, the reactive parts nearly cancel, which is partly the reason for the high 3rd harmonic magnification in the ac-bus voltages.

VI. Conclusions

A technique based on harmonic impedances has been used to determine the responses of six-pulse, current-controlled, ac/dc converters. The technique enables the computation of the converter's impedance (admittance) at the dc (ac) terminals.

Harmonic magnification factors have been defined and computed. High values of magnification imply the possibility of composite resonance. These factors have been used to determine the maximum impact of negative-sequence imbalance on the ac-bus voltage and dc current harmonics.

Acknowledgment

S. R. Naidu thanks the Brazilian Science Research Council (CNPq) for the award of a visiting fellowship. This research was carried out at the University of Wisconsin during S. R. Naidu's tenure as a visiting scholar.

References

[1] J. D. Ainsworth, "Harmonic instability between controlled static converters and a.c. networks," *Proc. Inst. Elect. Eng.*, vol. 114, pp. 949–957, July 1967.

[2] E. V. Larsen, D. H. Baker, and J. C. McIver, "Low-order harmonic interactions on AC/DC systems," *IEEE Trans. Power Delivery*, vol. 4, pp. 493–501, Jan. 1989.

[3] A. E. Hammad, "Analysis of second harmonic instability for the Chateauguay HVDC/SVC scheme," *IEEE Trans. Power Delivery*, vol. 7, pp. 410–415, Jan. 1992.

[4] P. Mattavelli and M. Perna, "Harmonic interaction on AC/DC systems: Effects of control actions," in *Proc. 7th IEEE Int. Conf. Harmonics Quality Power*, Las Vegas, NV, Oct. 16–17, 1996, pp. 501–506.

[5] E. V. Persson, "Calculation of transfer functions in grid controlled converter systems," *Proc. Inst. Elect. Eng.*, vol. 117, no. 5, pp. 989–997, May 1970.

[6] L. Hu and R. Yacamini, "Harmonic transfer through converters and hvdc links," *IEEE Trans. Power Electron.*, vol. 7, pp. 514–525, July 1992.

[7] A. R. Wood and J. Arrillaga, "Composite resonance; a circuit approach to the waveform distortion dynamics of an HVDC converter," *IEEE Trans. Power Delivery*, vol. 10, pp. 1882–1888, Oct. 1995.

[8] M. P. Bahrman, G. C. Brownell, K. J. Peterson, P. R. Shockley, and R. H. Lasseter, "DC system resonance analysis," *IEEE Trans. Power Delivery*, vol. 2, pp. 156–164, Jan. 1987.

[9] E. O. Brigham, *The Fast Fourier Transform*. Englewood Cliffs, NJ: Prentice-Hall, 1974.

[10] R. H. Lasseter, *EMTP Workbook IV*. Palo Alto, CA: Elect. Power Res. Inst., 1989.

S. R. Naidu is a Professor in the Department of Electrical Engineering at Federal University, Paraiba, Brazil. He received the Ph.D. degree in electrical engineering from the University of Liverpool, U.K., in 1975.

He was a Visiting Scholar with the University of British Columbia, Vancouver, and with the University of Wisconsin, Madison, from 1986 to 1988 and 2000 to 2001, respectively. His research interests include nonlinear circuits, electromagnetic transients, and electromagnetic field computation.

Robert H. Lasseter (F'92) received the Ph.D. degree in Physics from the University of Pennsylvania, Philadelphia, in 1971.

He was a Consulting Engineer with General Electric Co., Philadelphia, PA, until he joined the University of Wisconsin-Madison in 1980. His research interests include the application of power electronics to utility systems and technical issues which arise from the restructuring of the power utility system. This work includes interfacing micro-turbines and fuel cells to the distribution grid, control of power systems through FACTS controllers, use of power electronics in distribution systems, and harmonic interactions in power electronic circuits.

Dr. Lasseter is a Fellow of IEEE, an expert advisor to CIGRE SC14, and Chairman of IEEE Working Group on Distributed Generation.